Effects of Temperature on the FT NIR Raman Spectra of Fish Skin Collagen

Maria Połomska [1], Leszek Kubisz [2,*], Jacek Wolak [1] and Dorota Hojan-Jezierska [3]

[1] Institute of Molecular Physics, Polish Academy of Sciences, Smoluchowskiego 17, 60-179 Poznań, Poland; polomska@imfpan.pl (M.P.); wolak@ifmpan.poznan.pl (J.W.)

[2] Department of Biophysics, Chair of Biophysics, Poznań University of Medical Sciences, Grunwaldzka 6, 61-701 Poznań, Poland

[3] Department of of Hearing Healthcare Profession, Chair of Biophysics, Poznań University of Medical Sciences, Grunwaldzka 6, 61-701 Poznań, Poland; djeziers@ump.edu.pl

[*] Correspondence: lkubisz@ump.edu.pl

Abstract: The development of regenerative medicine turns attention toward native collagen as a biocompatible material. Particularly interesting is fish skin collagen, which is relatively easy to extract comparing mammalian tissues and free of some pathogens that are dangerous to humans. The paper presents results of IR Raman spectroscopy studies of silver carp (*Hypophthalmichthys molitrix*) skin collagen. As collagen properties result from its structure and conformation, both sensitive to temperature, FT NIR Raman spectroscopy is an excellent tool to characterize the molecular structure of fish skin collagen, particularly in temperature range typical for the manufacturing processes of biomedical products. Therefore, the Raman spectra were recorded in a temperature range of 300 to 403 K. The analysis of Raman spectra of prepared collagen films, particularly in the range of the bands related to amide I and amide III entities, showed a high content of α-helix and α-helix type molecular organization in fish skin collagen. Additionally, the secondary structure of the studied fish skin collagen is stable up to ~358 K. Heating to 403 K leads to irreversible changes in the molecular structure of fish skin collagen. It was found that the Raman spectrum of fish skin collagen preheated in this manner becomes similar to the spectrum of the collagen obtained from bovine Achilles tendon, whose secondary structure does not change up to 403 K.

Keywords: Raman spectroscopy; fish skin collagen; molecular structure; thermal stability

1. Introduction

Collagen is the main constituent of connective tissue in living organisms. Collagen is the basic structural and protective protein, constituting about 30% of the total protein content and more than 50% of the skin [1]. Collagen is responsible for the mechanical functions of the skin, its elasticity and tensile strength. It is an important element in the process of healing injuries, representing 50% of all proteins of a properly healing wound. The uncovering of collagen fibers in damaged tissues triggers a chain of cellular and biochemical reactions initiating the process of blood clotting and healing of tissues. This property of collagen is utilized in the process of homeostasis initiated by means of a collagen sponge applied on the wound [2–4].

The proper process of synthesis and maturation of collagen fibers has a significant influence on the final properties of the scar, its arrangement and strength. Therefore, exogenous collagen, which can additionally convey other substances, such as, e.g., antibiotics, is frequently used to treat wounds [5–8]. Moreover, collagen is a main component of many biomedical hybrid materials [9–11]. Exogenous collagen is applied in tissue engineering and cosmetology. Additionally, some conclusions have been drawn on the correlation of primary fish collagen structure and conformation to film-forming abilities [12]. Medical and cosmetic applications of collagen result from a variety of forms in which it is available

and its ability to bond with other polymers, both natural and synthetic [13,14]. Collagen, including that of animal origin, which is recognized by the organism as its component and not a foreign matter [11,15–18], is characterized by a high degree of biocompatibility [15]. The biocompatibility of collagen is connected with its structure and conformation of molecules. This fact justifies the importance of research into its structure and thermal stability.

Fish collagen, contrary to mammalian collagen, is usually free of some pathogens dangerous to humans. The advantages of fish collagen involve ethical issues related to customs and religions and economic considerations, which are equally important, as fish waste products are a cheap source of collagen [19].

Thus, attention was turned towards fish collagen due to its native structure maintained during the extraction process [20–22]. Collagens originating from different fish species differ in their denaturation temperature. Generally, the lower the temperature of the feeding ground (water) for fish, the lower the denaturation temperature of collagen macromolecules. Particularly interesting, from the point of view of economy, is silver carp (*Hypophthalmichthys molitrix*), a freshwater fish. The denaturation temperature of silver carp skin collagen is reported to be either 302 K [1] or 307 K [3,23,24] depending on the experimental technique. The closer the denaturation temperature of fish skin collagen to mammalian collagen, the higher the potential in supplementing/replacing the skin of land vertebrates as a collagen source and substituting mammalian collagen. Moreover, fish skin collagen extraction is easier and has a higher yield comparing the extraction from mammalian skin [17,25,26].

The basic structural unit of collagen and collagen structure is described elsewhere [27–32]. Collagen polypeptide chains are rich in glycine (Gly), proline (Pro) and 3hdroxyproline (Hyp) (Figure 1), linked together in the characteristic pattern X_{Pro}-Y_{Hyp}-Gly [29].
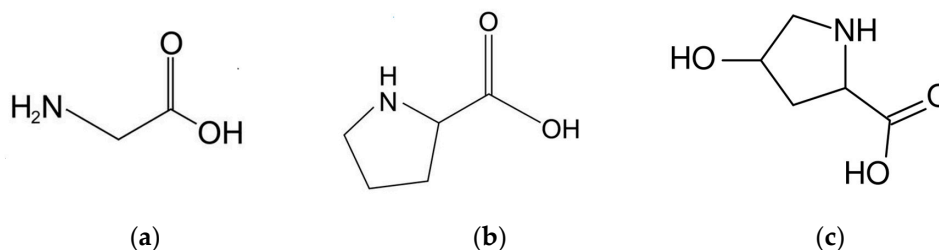

(a)   (b)   (c)

Figure 1. Schematic model of glycine (**a**), proline (**b**) and hydroxyproline (**c**).

Other amino acids residues, such as alanine, lysosine and tyrosine, may occur in the X or Y locations of the polypeptide chain. In the α-chain of fibrous collagen, about 25% of amino acids are proline and hydroxyproline. They stabilize the triple-helical structure and effectively block internal rotations of collagen chains at these sites [33]. Moreover, hydroxyproline is an important amino acid in maintaining thermal stability of collagen molecules [34,35]. The most common secondary structure in collagen type I is the α-helix forming a triple helix along with the β-sheet and irregular conformation [36,37].

The triple helix structure is upheld mainly by hydrogen bonds between the glycine - NH group and carbonyl group C=O of residues of another polypeptide chains. Additionally, the triple helix's stability is due to hydrogen bonds between the CαH group from glycine and C=O and hydrogen bonds with water molecules.

The tree of hydrogen bonds is essential for maintaining the triple helix's stability. On the contrary, its absence leads to a variety of pathological situations [32,38]. The collagen helix is additionally stabilized by van der Waals forces, along with hydrophobic and electrostatic short range interactions [39].

The secondary structure of native collagen can be affected by different factors such as temperature, mechanical forces and chemicals [40–45]. Any deformation in colla-

gen/protein structure and conformation can be followed by means of Raman spectroscopy, which is particularly useful for this purpose. Any alteration/variation in collagen molecules is noticed in the shift of the position of Raman bands, their intensity and spectral width. The aim of the study was to characterize the secondary structure of silver carp skin collagen in terms of exposure to temperature by means of Fourier transform near IR Raman spectroscopy. NIR Raman spectroscopy appears to be an extremely useful in biomaterials studies. Using laser excitation with wavelength of 1064 nm, beyond the range of electronic absorption, we avoid fluorescence effects. Additionally, lower energy excitation allows us to avoid decomposition (e.g., thermal, photochemical, chemical) of the biomaterials during study. As the reference material, bovine Achilles tendon collagen was used.

2. Materials and Methods

The collagen gel used in the experiment was obtained from silver carp (*Hypophthalmichthys molitrix)* skin (FS collagen) Collagen was purchased from Collagen Active Science Sp. z o. o. Poznan, Poland.The FS collagen obtained by means of the method presented in [21] most probably exhibits a triple helix conformation which is unique to living organisms, which was verified by viscosity measurements and electrophoresis [3,46,47].

Collagen native conformation was determined by means of temperature dependence of viscosity using the Ubbelohde viscometer, in the temperature range of 293–333 K. The denaturation temperature was established as (306.3 ± 1.5) K [3,24,47]. The molecular weight characteristics found by electrophoresis showed two distinct lines at ~130 and ~200 kDa, related to α- and β-chains, respectively [44]. The amino acid content can be found elsewhere [46].

Collagen gel was dissolved in water and the acquired 10% solution was poured into a Petri dish and dried at room temperature. Obtained films were used in further studies. Raman spectra were recorded with a Bruker IFS66FT IR spectrometer equipped with an FRA106 Raman module. The samples were excited by a diode pumped Nd:YAG laser operated at $\lambda = 1064$ nm with output power of ~50 mW. Raman spectra were measured in the 303–403 K range of temperature using a Linkam cooling–heating stage in 180° geometry. The temperature range of approximately 300–400 K covers the temperature range expected in many biomedical applications as well as collagen stability against temperature [48].

Moreover, the application of IR radiation permitted us to avoid any effect of UV radiation on collagen structure [49].

The molecular structure and the temperature effects on the secondary structure of fish skin (FS) collagen were compared with bovine Achilles tendon (BAT) collagen purchased from Sigma-Aldrich, Poland. Its amino acid composition can be found in [50].

3. Results and Discussion

3.1. Raman Spectra of FS and BAT Collagen Measured at Room Temperature

The Raman spectra of FS and BAT collagen recorded at 303 K are presented in Figure 2.

Table 1 presents the assignment of the Raman bands for FS and BAT type collagen at room temperature. To assign the Raman bands of samples used in this study, the results of vibrational studies of different samples containing different kinds of collagen as well as proline, hydroxyproline and glycine separately were utilized [35–37,45,51–59].

In the Raman spectra of collagen, one can distinguish four principal frequency ranges: the first at 200–600 cm^{-1}, assigned to the vibrations of the triple helix [44,59], the second at 800–1200 cm^{-1}, assigned mainly to the vibration of proline and hydroxyproline as well as secondary structure of collagen, and the third at 1200–1750 cm^{-1}, where the bands related to amide I and amide III vibrations were observed. The fourth frequency range from 2800 to 3200 cm^{-1} presents the band related to CH_2 group vibrations.
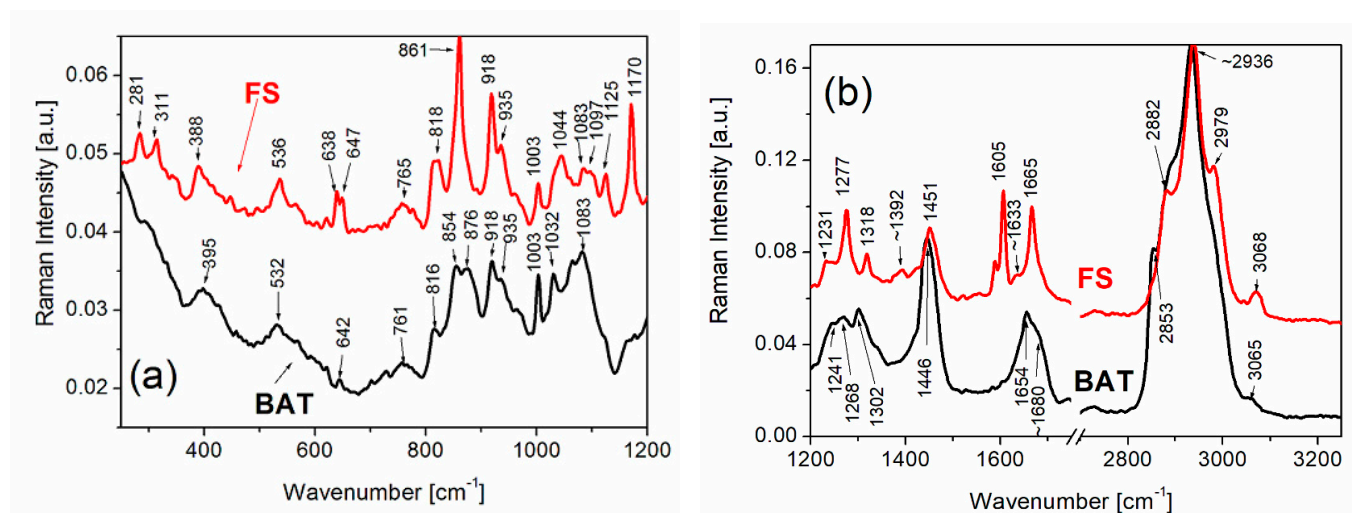
Figure 2. Raman spectra of FS and BAT types of collagen in the range from 250 to 1200 cm^{-1} (**a**), in the range of amide I, amide III and the range of CH$_2$ vibrations (**b**). Raman spectra were recorded at 303 K.

Table 1. Assignment of the Raman bands of FS and BAT types of collagen at room temperature.

FS Band Position/cm^{-1}	BAT Band Position/cm^{-1}	Assignment	Assignment
282 w	292 vw		3-helix
314 w	307 vw		3-helix
388 vw	396 w		
535 w	530 w	δ(CCN)	
639 w	644 vw	δ,ω(COO$^-$)	
649 w			
760 w	760 w	ν(CCO)	
813 w	815 w	ν(COC), ν(CC)	
822 w			
850 wsh	854 m	ν(COC), ν(CC)	Pro
861 m			
870 wsh	874 m	ν(CC)	Hyp
918 m	918 m	ν(C-COO$^-$)	α-helix
935 m	935 m	ν(CC)	α-helix
962 w	964 w		
975 w	974		
1003 w	1002 m	ν(CC) aromatic ring	phenylalanine, tyrosine, tryptophane
1029 wsh	1030 m	ν(CCN)	phenylalanine
1045 w	1042 wsh		β-sheet
1060 sh	1064 m	ω(CH$_2$)	β-sheet
1085 w	1082 m	ν(CN)	
1096 w	1096 msh	ν(CN)	
1124	1123 msh		

Table 1. *Cont.*

FS Band Position/cm^{-1}	BAT Band Position/cm^{-1}	Assignment	Assignment
1171 m		δ(CH), ν(CCC) out-of-phase	tyrosine
1233 m		ν(CN), δ(CH), δ(NH)	
	1245 ssh	δ(NH)	disordered (amide III)
1275 m	1270 s	δ(NH)	α-helix (amide III)
	1301 s		
1318 w	1318 sh	γ(CH$_2$)	
1340 wsh	1340 msh	δ(CH$_2$)	
1391 vw		δ(CH$_2$), ν(COO$^-$)	
1449 s	1445 s	δ(CH$_2$)	
1588 wsh	1583 s	ν(CCH) aromatic ring	
1607 s	1604	ν(CCH) aromatic ring	
1633 wsh		ν(C=O)	3-helix
1666 s	1656 s	ν(C=O)	α-helix (amide I)
	1671 s		β-sheet (amide I)
	1680		disordered (amide I)
2861 ssh	2853 ssh	ν_{as}(CH$_2$)	
	2888 ssh		
2938 vs	2934 vs	ν_s (CH$_2$)	
2982 ssh			
3071 w		ν(C=CH)	

Abbreviations: s: strong, m: medium, w: weak, v: very, sh: shoulder, ν: stretching, δ: in plane bending symmetric, γ: in plane bending antisymmetric, ω: out of plane bending symmetric.

The Raman lines at 282 and 314 cm^{-1} are clearly visible for FS collagen, whereas similar lines at ~292 and 307 cm^{-1} for BAT collagen are broadened and exhibit low intensities. Some authors [41,53] assign the lines in the range 200 to 400 cm^{-1} to the vibrations related to a triple helicity of the collagen. A significant difference between FS collagen and BAT collagen is observed in the frequency range 830–900 cm^{-1}. The doublet of lines at 854 and 874 cm^{-1} for BAT collagen is assigned to δ(CCH) aromatic and ν(CC) proline and hydroxyproline vibrations, respectively. In the case of FS collagen, one intense band with weak shoulders is observed at 861 cm^{-1}. After deconvolution of the band, the shoulders occur at ~854 cm^{-1} and ~870 cm^{-1}. The band centered at 861 cm^{-1} may be assigned to the vibrations related to tyrosine. The shoulders with low intensities at ~854 and ~870 cm^{-1} may be related to the vibrations of proline and hydroxyproline. The remaining Raman bands occurring in this frequency range appear in similar positions and are characterized by similar intensities, both for BAT and FS.

As was discussed in the earlier papers [42,43], the lines related to C-C stretching vibrations in the range 890 to 1060 cm^{-1} may also characterize the secondary structure of collagen. The lines at 918 and 936 cm^{-1} are characteristic of α-helices and the lines in the range from 1020 to 1060 cm^{-1} are related to β-sheet structure. A gradual loss of these structures leads to a broadening and weakening in the intensity of the bands which are assigned to these vibrations [43]. The Raman band positions of these vibrations are similar for FS and BAT types of collagen. There are, however, some differences in the ratio of the band intensities. The band at 918 cm^{-1} for FS exhibits higher intensity compared to the same line for BAT. It could also be related to a higher content of the α-chain conformation

in FS. Another difference between the Raman spectra of BAT and FS collagen appears for the line at 1171 cm^{-1}, which is assigned to ν(CCC) out-of-phase vibration related to the vibrations of tyrosine residue. The line, which is sharp and intense for FS collagen, has very low intensity for BAT.

The vibrations of amide I and amide III are most sensitive to changes in the conformation of the secondary structures of collagen. The vibrations related to these molecular groups appear in the spectral range from 1200–1750 cm^{-1}. The bands between 1200 and 1350 cm^{-1} are assigned to the vibrations of amide III, where the modes related to C-N stretching and N-H in-plane bending vibrations of the peptide bond as well as contributions from C-C stretching and C=O in-plane bending vibrations exist. The bands located in the range around 1260–1300 cm^{-1} may be responsible for the α-helix conformation, whereas the bands between 1240 and 1250 cm^{-1} could be related to both random coil and β-sheet structures [43].

The bands revealed in the range ~1600–1680 cm^{-1} are mainly assigned to the stretching vibrations C=O of the peptide bond and the bending vibrations of the N-H group. The bands of amide I can characterize the hydrogen bonds of diverse structures. These diverse hydrogen bonds in the polypeptide chain are responsible for the type of the secondary structure of the protein that is an α-helix arranged in a spiral which is stabilized by hydrogen bonds between the oxygen of the C=O group of one amino acid and nitrogen of a second amino acid located four positions away. The β-sheet is conformation which should contain a minimum of two strands and is stabilized by hydrogen bonds between the C=O group of one strand and the NH group of the another strand as well as disordered structures. The Raman band assigned to amide I of FS collagen consists of a narrow line at ~1666 cm^{-1} and a shoulder at ~1633 cm^{-1}. On the basis of the previous Raman studies on collagen [37,57], this band can be attributed to a significant content of α-helix structures. In the case of BAT collagen, a wide band of amide I having the local maximum at ~1655 cm^{-1}, along with extra shoulders at ~1671 cm^{-1} and ~1680 cm^{-1}, was observed. Such a wide, complex band related to amide I of BAT collagen can suggest that it contains α-helix structures as well as β-sheet and other disordered structures. The most intense bands presented in the range 2800–3200 cm^{-1} belong to the stretching vibrations of the CH$_2$ group and are similar for both FS and BAT types of collagen.

3.2. Temperature Effect on the FS Collagen

Temperature studies of Raman spectra of FS and BAT collagen were carried out in the temperature range from 303 K to 403 K. In Figure 3a,b, temperature changes of FS collagen and BAT collagen Raman spectra are presented, respectively. Raman spectra of FS collagen do not change up to T $\cong$ 353 K, and above 353 K Raman spectra undergo irreversible change. The most significant changes are observed for the lines at 860, ~918, 935, 1171 cm^{-1} and for the bands related to amide I and amide III vibrations. The sharp line at 860 cm^{-1} in the spectrum at 303 K, assigned to tyrosine, is significantly less intense at 403 K (Figure 4a). The doublet of lines at 918 and 935 cm^{-1}, assigned to α-helix conformation, shows a considerable decrease in their intensities at 403 K. The most significant changes in high temperature are observed for the bands related to both amide I and amide III vibrations. A substantial shift of the band at 1274 cm^{-1} to ~1270 cm^{-1} (Figure 5a) assigned to the α-helix may indicate its considerable decrease and an increase in the content of both β-sheets and the disordered part of the polypeptide chain. On the other hand, in the part of the Raman spectrum related to the vibrations of amide I (Figure 5c), one can observe a shift of a narrow band centered at 1666 cm^{-1} to a higher frequency at ~1670 cm^{-1}. Moreover, a decreasing intensity of the line suggests a reduction in the content of α-helix conformation and an increase in the content of the β-sheet phase. We can also observe a significant widening of Raman bands, indicating increased structural disorder (Figure 5b).
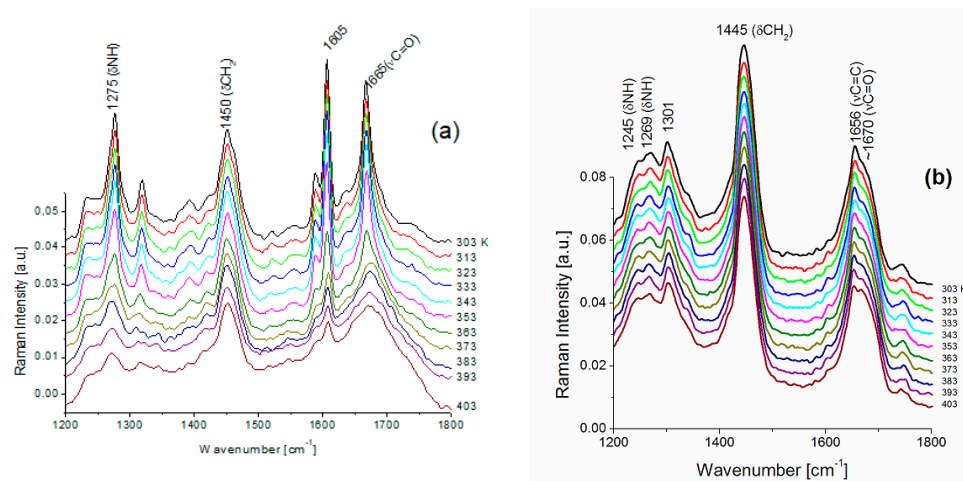
Figure 3. Temperature changes of Raman spectra for FS collagen (**a**) and BAT collagen (**b**) in the frequency range of amide III and amide I vibrations.
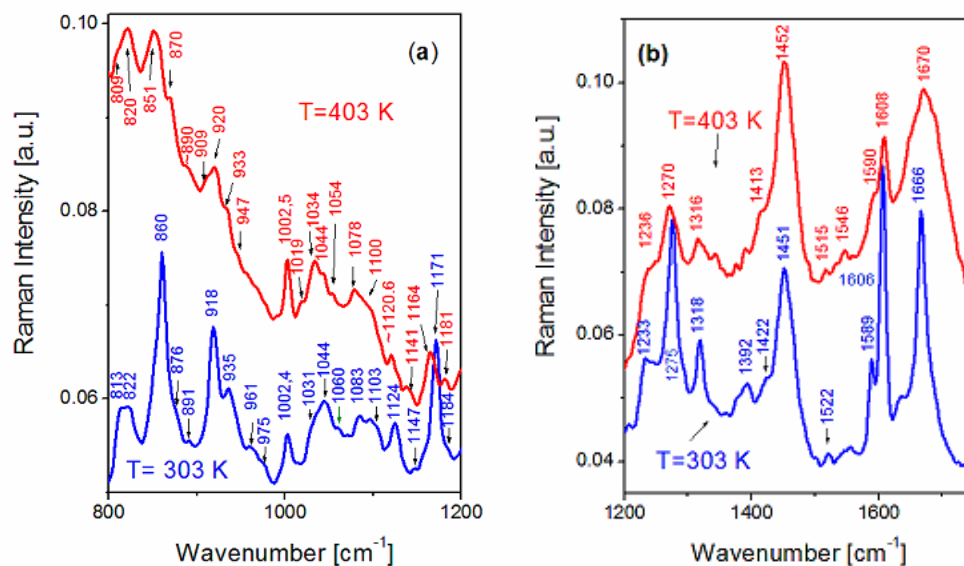

Figure 4. Comparison of Raman spectra of FS collagen measured at 303 K and 403 K in the frequency ranges 800–1200 cm^{-1} (**a**) and 1200–1750 cm^{-1} (**b**).
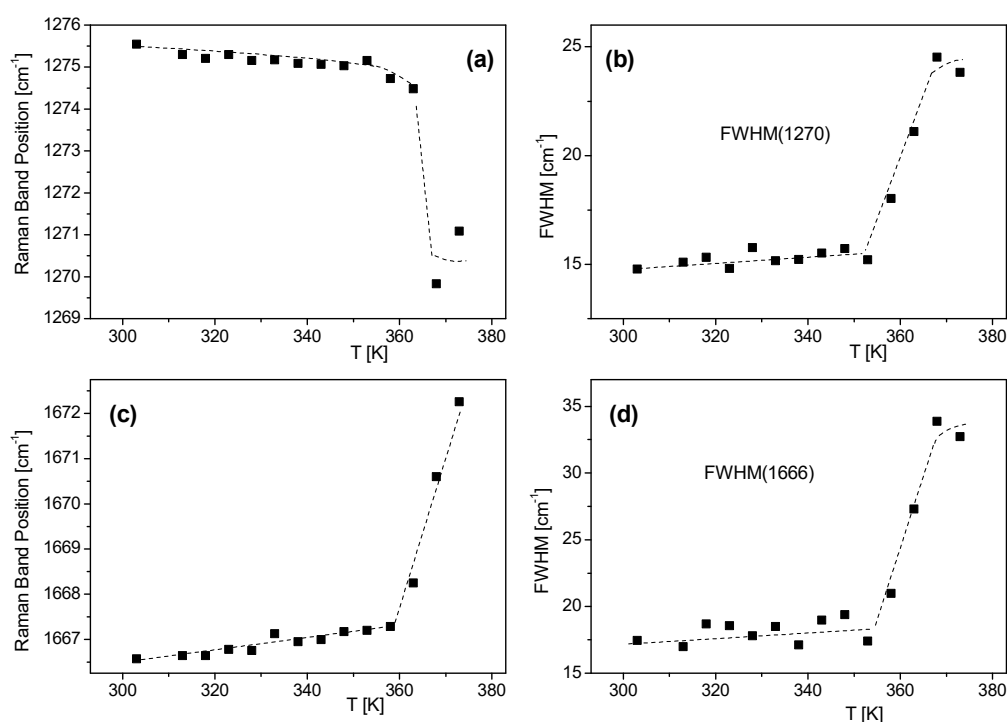
Figure 5. Temperature dependence of the Raman band position of FS related to amide III vibration (**a**) and its spectral width (**b**), amide I vibration (**c**) and its spectral width (**d**). The lines are guides for the eye.

To conclude, the temperature studies of the Raman spectra of FS collagen revealed conspicuous changes occurring in the ~358 K to ~363 K temperature range. Heating of FS collagen to 403 K causes irreversible changes in its secondary structure.

Comparing the Raman spectra of BAT and FS collagen measured at 403 K (Figure 6), one can see their striking similarity, whereas at room temperature considerable differences can be observed (see Figure 2).
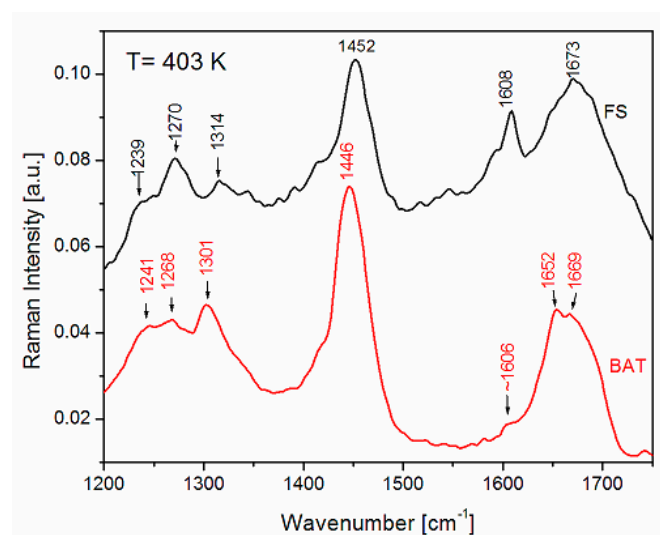

Figure 6. Comparison of Raman spectra of FS and BAT collagen in the range of amide I and amide III vibrations measured at 403 K.

Temperature studies of Raman spectra changes in BAT collagen showed that the character of Raman spectra does not undergo any change in the temperature range from 300 K to 403 K (Figures 3b and 7). Additionally, the Raman band positions change linearly with increasing temperature (Figure 8), not exhibiting any anomalous behavior.
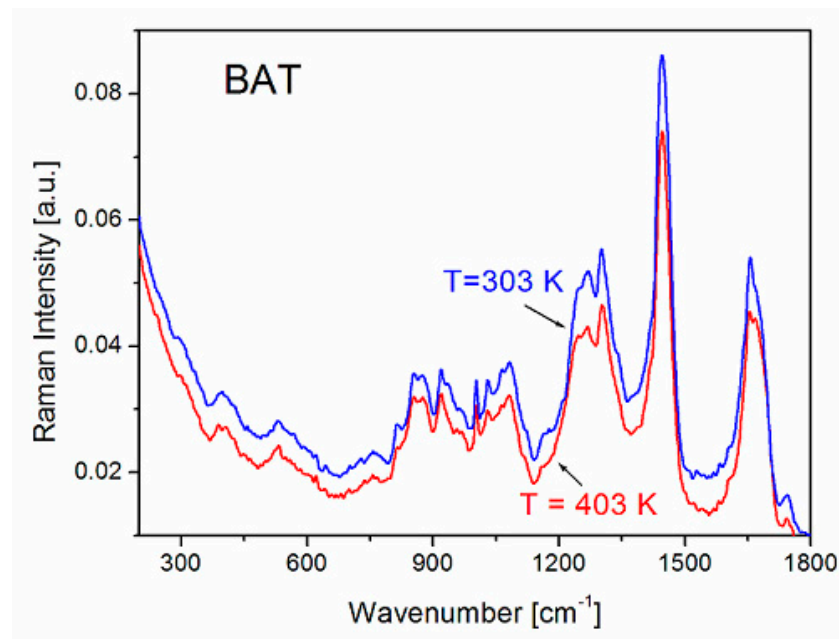
Figure 7. Comparison of the Raman spectra of BAT collagen measured at 303 K and 403 K.
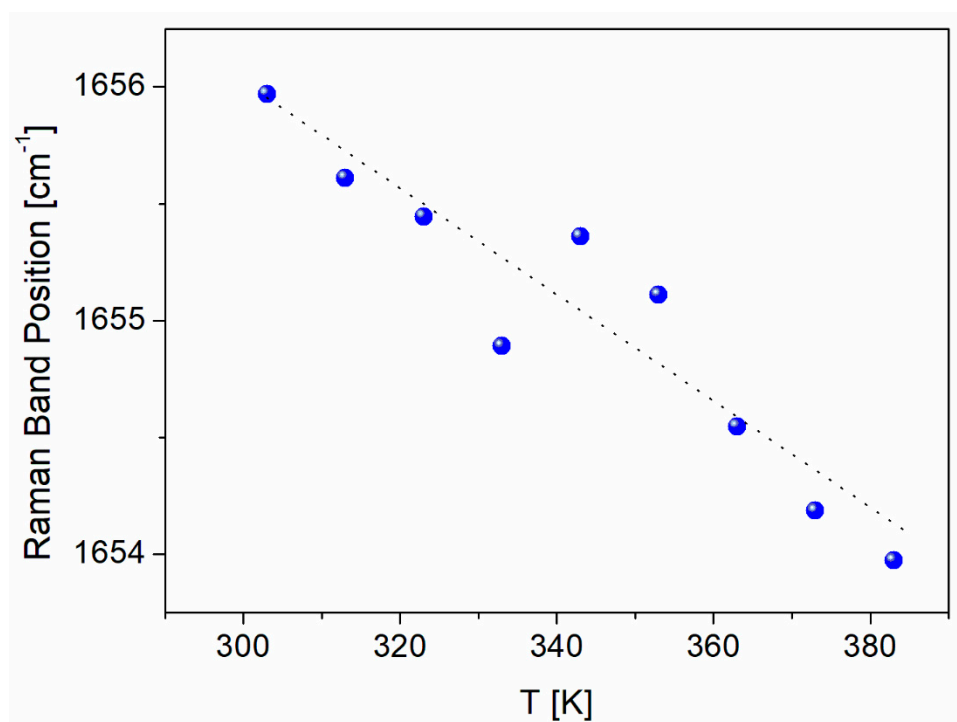

Figure 8. Temperature dependence of the Raman band position of BAT collagen related to amide I vibration. The line is a guide for the eye.

Analyzing the thermal changes in the amide groups for both FS and BAT types of collagen, we compare the Raman intensity ratios of the most intense bands at ~1270 cm^{-1} (precisely ~1275 cm^{-1} for FS and ~1270 cm^{-1} for BAT) for amide III and ~1660 cm^{-1} (1666 cm^{-1} for FS and ~1656 cm^{-1} for BAT) for amide I with the intensity of the band at ~1450 cm^{-1}. The band at ~1450 cm^{-1} is related to the CH$_2$ bending vibration, which is practically insensitive to the secondary structure. Table 2 presents the Raman band intensity ratios at 303 K and 403 K for both types of collagen.

Table 2. Raman intensity ratios of amide I and amide III bands to Raman intensity of CH_2 band for FS and BAT collagens.

	Amide I $I_{(\sim 1660)}/I_{(\sim 1450)}$	Amide III $I_{(\sim 1270)}/I_{(\sim 1450)}$	Amide I $I_{(\sim 1660)}/I_{(\sim 1450)}$	Amide III $I_{(\sim 1270)}/I_{(\sim 1450)}$
Temperature	303 K		403 K	
FS	1.56	1.16	0.65	0.49
BAT	0.62	0.39	0.63	0.36

As shown earlier, the Raman spectra of BAT collagen do not undergo any change up to 403 K. The intensity ratios of the Raman bands characteristic of α-helix frequencies of amide I and amide III to the CH_2 bending band presented in Table 2 are nearly the same for 303 K and 403 K. However, in the case of FS collagen, these dependences change considerably. At 303 K, the intensity ratios of the bands assigned to the vibrations of α-helix conformation are nearly three times higher for amide I and almost four times higher for amide III, compared with BAT collagen, while at 403 K the values are comparable.

4. Conclusions

The analysis of the recorded Raman spectra of fish skin collagen at room temperature revealed a relatively high content of α-helix structure in a film made of collagen gel. The high intensity of the bands of amide I and amide III at ~1666 cm^{-1} and ~1274 cm^{-1}, respectively, suggested a significant content of α-helix structure in the studied material. The intensities of the above bands were much higher than the intensities of the corresponding bands for the BAT collagen.

The effect of temperature on the Raman spectra of FS collagen was insignificant up to the temperature 358 K. Above this temperature, the content of α-helix structure was reduced and beneficial to the β-sheet structure and other disordered structures. From this temperature, the Raman spectrum of FS collagen resembled the Raman spectrum of BAT collagen. Therefore, one could conclude that FS collagen is thermally stable up to ~358 K and maintained its native structure. Opposite to fish skin collagen, studies on temperature effects on Raman spectra of BAT collagen did not reveal any change in the secondary structure up to temperature 403 K.

These results coincide with the results of studying the thermal stability of FS collagen foil by means of the DSC method presented in [40,41]. It was shown in these works that the thermal stability temperature of the foil collagen from swim bladders obtained from a variety of fish is 338.9–347.8K [60], whereas for the collagen films from silver carp skin it is 350K or 352K [61,62]. This indicates an ideal agreement of denaturation temperature of collagen foil determined by means of the DSC method with the temperature at which the changes in the secondary structure of FS collagen revealed by Raman spectroscopy were observed in the present work.

A high content of α-helix structure in fish skin collagen suggests its high biocompatibility and a variety of possible applications in regenerative medicine and cosmetology.

References

1. de Melo Oliveira, V.; Assis, C.R.D.; Costa, B.D.A.M.; de Araujo Neri, R.C.; Monte, F.T.D.; da Costa Vasconcelos, H.M.S.; Franca, R.C.P.; Santos, J.F.; Bezerra, R.d.S.; Porto, A.L.F. Physical, biochemical, densitometric and spectroscopic techniques for characterization collagen from alternative sources: A review based on the sustainable valorization of aquatic by-products. *J. Mol. Struct.* **2021**, *1224*, 129023. [CrossRef]
2. Manon-Jensen, T.; Kjeld, N.G.; Karsdal, M.A. Collagen-mediated hemostasis. *J. Thromb. Haemost.* **2016**, *14*, 438–448. [CrossRef]
3. Kubisz, L.; Hojan-Jezierska, D.; Szewczyk, M.; Majewska, A.; Kawałkiewicz, W.; Pankowski, E.; Janus, M.; Cwajda-Białasik, J.; Mościcka, P.; Jawień, A. In vivo electrical impedance measurement in human skin assessment. *Pure Appl. Chem.* **2019**, *91*, 1481–1491. [CrossRef]
4. Park, K.H.; Kwon, J.B.; Park, J.H.; Shin, J.C.; Han, S.H.; Lee, J.W. Collagen dressing in the trement of diabetic foot ulcer: A prospective, randomized, placebo-controlled, single-center study. *Diabetes Res. Clin. Pract.* **2020**, *156*, 107861. [CrossRef] [PubMed]
5. Liu, X.; Zheng, C.; Luo, X.; Wang, X.; Jiang, H. Recent advances of collagen-based biomaterials: Multi-hierarchical structure, modification and biomedical applications. *Mater. Sci. Eng.* **2019**, *99*, 1509–1522. [CrossRef]
6. Chong, C.; Wang, Y.; Fathi, A.; Parungao, R.; Maitz, P.K.; Li, Z. Skin wound repair: Results of a pre-clinical study to evaluate electropsun collagen–elastin–PCL scaffolds as dermal substitutes. *Burns* **2019**, *45*, 1639–1648. [CrossRef] [PubMed]
7. Lukáč, P.; Hartinger, J.M.; Mlček, M.; Popková, M.; Suchý, T.; Šupová, M.; Zavora, L.; Adamkova, V.; Benakova, H.; Slanar, O. A novel gentamicin-releasing wound dressing prepared from freshwater fish Cyprinus carpio collagen cross-linked with carbodiimide. *J. Bioact. Compat. Polym.* **2019**, *34*, 246–262. [CrossRef]
8. Cwajda-Białasik, J.; Mościcka, P.; Szewczyk, M.T.; Hojan-Jezierska, D.; Kawałkiewicz, W.; Majewska, A.; Janus-Kubiak, M.; Kubisz, L.; Jawień, A. Venous leg ulcers treated with fish collagen gelin a 12-week randomized single-centre study. *Adv. Dermatol. Allergol.* **2021**, *38*, 1–9. [CrossRef]
9. Lotz, C.; Schmid, F.F.; Oechsle, E.; Monaghan, M.G.; Walles, H.; Groeber-Becker, F. Cross-linked collagen hydrogel matrix resisting contraction to facilitate full-thickness skin equivalents. *ACS Appl. Mater. Interfaces* **2017**, *9*, 204. [CrossRef]
10. Miri, A.K.; Muja, N.; Kamranpour, N.O.; Lepry, W.C.; Boccaccini, A.R.; Clarke, S.A.; Nazhat, S.N. Ectopic bone formation in rapidly fabricated acellular injectable dense collagen-bioglass hybrid scaffolds via gel aspiration-ejection. *Biomaterials* **2016**, *85*, 128–141. [CrossRef]
11. Sionkowska, A.; Skrzyński, S.; Śmiechowski, K.; Kołodziejczak, A. The review of versatile application of collagen. *Polym. Adv. Technol.* **2017**, *28*, 4–9. [CrossRef]
12. Chen, L.T.S.; Su, W.; Weng, W.; Osako, K.; Tanaka, M. Physicochemical properties and film-forming ability of fish skin collagen extracted from different freshwater species. *Process. Biochem.* **2015**, *50*, 148–155.
13. Bardakova, K.N.; Grebenik, E.A.; Minaev, N.V.; Churbanov, S.N.; Moldagazyeva, Z.; Krupinov, G.E.; Kostjuk, S.V.; Timasheva, P.S. Tailoring the collagen film structural properties via direct laser crosslinking of star-shaped polylactide for robust scaffold formation. *Mater. Sci. Eng.* **2020**, *107*, 110300. [CrossRef] [PubMed]
14. Szumała, P.; Jungnickel, C.; Kozłowska-Tylingo, K.; Jacyna, B.; Cal, K. Transdermal transport of collagen and hyaluronic acid using water in oil microemulsion. *Int. J. Pharm.* **2019**, *572*, 118738. [CrossRef] [PubMed]
15. An, B.; Lin, Y.S.; Brodsky, B. Collagen interactions: Drug design and delivery. *Adv. drug Deliv. Rev.* **2016**, *97*, 69–84. [CrossRef]
16. Chowdhury, S.R.; Busra, M.F.M.; Lokanathan, Y.; Ng, M.H.; Law, J.X.; Cletus, U.C.; Idrus, R.B.H. Collagen type I: A versatile biomaterial. *Nov. Biomater. Regen. Med.* **2018**, *1077*, 389–414.
17. Blidi, E.; del Omari, N.; Balahbib, A.; Ghchime, R.; del Menyiy, N.; Ibrahimi, A.; Kaddour, K.B.; Bouyahya, A.; Chokairi, O.; Barkiyou, M. Extraction Methods, Characterization and Biomedical Applications of Collagen: A Review. *Biointerface Res. Appl. Chem.* **2021**, *11*, 13587–13613. [CrossRef]
18. Salvatorea, L.; Gallob, N.; Natalia, M.L.; Campaa, L.; Lunettib, P.; Madaghieleb, M.; Blasib, F.S.; Corallob, A.; Capobiancoc, L.; Sannino, A. Marine collagen and its derivatives: Versatile and sustainable bio-resources for healthcare. *Mater. Sci. Eng.* **2020**, *113*, 110963. [CrossRef]
19. Rahman, A. Collagen of Extracellular Matrix from Marine Invertebrates and Its Medical Applications. *Mar. Drugs* **2018**, *16*, 118. [CrossRef]
20. Jayaraman, A.; Price, C.; Sullivan, M.O.; Kiick, K.L. Collagen-Peptide-Based Drug Delivery Strategies. *Technol. Innov.* **2020**, *21*, 1–20. [CrossRef]
21. Przybylski, J.E.; Siemaszko-Przybylska, K. Patent 190737 Patent Office, Poland. 2002.
22. Sun, J.; Zhang, J.; Zhao, D.; Xue, C.; Liu, Z.; Mao, X. Characterization of turbot (*scophthalmus maximus*) skin and the extracted acid-soluble collagen. *J. Ocean Univ. China* **2019**, *18*, 687–692. [CrossRef]
23. Rodziewicz-Motowidło, S.; Śladewska, A.; Mulkiewicz, E.; Kołodziejczyk, A.; Aleksandrowicz, A.; Miszkiewicz, J.; Stepnowski, P. Isolation and characterization of a thermally stable collagen preparation from the outer skin of the silver carp Hypophthalmichthys molitrix. *Aquaculture* **2008**, *285*, 130–134. [CrossRef]
24. Janus, M.; Pankowski, E.; Hojan-Jezierska, D.; Kubisz, L. Study of fish skin collagen by viscosimetric method. In Proceedings of the 24th Annual World Forum on Advanced Materials, Poznań, Poland, 9–13 May 2016; pp. 76–77.
25. Yunoki, S.; Suzuki, T.; Takai, M. Stabilization of low denaturation temperature collagen from fish by physical cross-linking methods. *J. Biosci. Bioeng.* **2003**, *96*, 575–577. [CrossRef]

26. Jafari, H.; Lista, A.; Siekapen, M.M.; Ghaffari-Bohlouli, P.; Nie, L.; Alimoradi, H.; Shavandi, A. Fish Collagen: Extraction, Characterization, and Applications for Biomaterials Engineering. *Polymers* **2020**, *12*, 2230. [CrossRef] [PubMed]

27. Bella, J.; Eaton, M.; Brodsky, B.; Berman, H.M. Crystal and molecular structure of a collagen like peptide at 1.9 Å resolution. *Science* **1994**, *266*, 75–81. [CrossRef] [PubMed]

28. Bella, J.; Berman, H.M. Crystallographic evidence for Cα–H··· O= C hydrogen bonds in a collagen triple helix. *J. Mol. Biol.* **1996**, *264*, 734–742. [CrossRef] [PubMed]

29. Okuyama, K.; Xu, X.; Iguchi, M.; Noguchi, K. Revision of collagen structure. *Biopolymers* **2005**, *84*, 181–191. [CrossRef]

30. Gelse, K.; Pöschl, E.; Aigner, T. Collagen-structure, function, and biosynthesis. *Adv. Drug Del. Rev.* **2003**, *55*, 1531–1546. [CrossRef]

31. Shoulders, M.D.; Raines, R.T. Collagen structure and stability. *Annu. Rev. Biochem.* **2009**, *78*, 929–958. [CrossRef]

32. Bonifacio, A.; Sergo, V. Effects of sample orientation in Raman microspectroscopy of collagen fibers and their impact on the interpretation of the amide III band. *Vib. Spectr.* **2010**, *53*, 214–217. [CrossRef]

33. Vogel, A.; Venugopalan, V. Mechanisms of pulsed laser ablation of biological tissues. *Chem. Rev.* **2003**, *103*, 577–644. [CrossRef]

34. Improta, R.; Benzi, C.; Barone, V. Understanding the role of stereelectronic effects in determining collagen stability. I. A quantum mechanical study of proline, hydroxyproline, and fluoroproline dipeptide analogues in aqueous solution. *J. Am. Chem. Soc.* **2001**, *123*, 12568–12577. [CrossRef] [PubMed]

35. Carcamo, J.J.; Aliaga, A.E.; Clavijo, R.E.; Garrido, C.; Gomez-Jeria, J.S.; Campos-Vallette, M.M. Proline and hydroxyproline deposited on silver nanoparticles. A Raman, SERS and theoretical study. *J. Raman Spectr.* **2011**, *439*, 750–755. [CrossRef]

36. Overman, S.A.; Thomas, G.J., Jr. Amide modes of the α-Helix:Raman Spectroscopy of Filamentous Virus fd containind peptide ¹³C and ²H labels in coat protein subunits. *Biochemistry* **1998**, *37*, 5654–5665. [CrossRef] [PubMed]

37. Gullekson, K.; Lucas, L.; Hewitt, K.; Kreplak, L. Surface sensitive Raman spectroscopy of collagen I fibrils. *Biophys. J.* **2011**, *100*, 1837–1845. [CrossRef] [PubMed]

38. Jenkins, C.L.; Bretscher, L.E.; Guzei, I.A.; Raines, R.T. Effect of 3-hydroxyproline residues on collagen stability. *J. Am. Chem. Soc.* **2003**, *125*, 5422–5427. [CrossRef] [PubMed]

39. Wisniewski, M.; Sionkowska, A.; Kaczmarek, H.; Lazare, S.; Tokarev, V.; Belin, C. Spectroscopic study of a KrF excimer laser treated surface of the thin collagen films. *J. Photochem. Photobiol. A Chem.* **2007**, *188*, 192–199. [CrossRef]

40. Renugopalakrishnan, V.; Carreira, L.A.; Collette, T.W.; Dobbs, J.C.; Chandraksasan, G.; Lord, R.C. Non-uniform triple helical structure in chick skin type I collagen on thermal denaturation: Raman spectroscopic study. *Z. Naturforsch.* **1998**, *53*, 383–388. [CrossRef]

41. Careche, M.; Herrero, A.M.; Rodriguez-Casado, A.; del Mazo, M.L.; Carmona, P. Structural changes of hake (*Merluccius merluccius* L.) fillets: Effects of freezing and frozen storage. *J. Agric. Food Chem.* **1998**, *47*, 952–959. [CrossRef]

42. Herreiro, A.M.; Carmona, P.; Careche, M. Raman spectroscopic study of structural changes in hake (*Merluccius merluccius* L.) muscle proteins during frozen storage. *J. Agric. Food Chem.* **2004**, *52*, 2147–2153. [CrossRef]

43. Herrero, A.M. Raman spectroscopy for monitoring protein structure in muscle food system. *Crit. Rev. Food Sci. Nutr.* **2008**, *48*, 512–523. [CrossRef]

44. Kumar, R.; Sripriya, R.; Kumar, M.S.; Sehgal, P.K. Physical characterization of succinylated type I collagen by Raman spectra and MALDI-TOF/MS and in vitro evaluation for biomedical application. *J. Mol. Struct.* **2011**, *994*, 117–124. [CrossRef]

45. Carcamo, J.J.; Aliaga, A.E.; Clavijo, R.E.; Branes, M.R.; Campos-Vallette, M.M. Raman study of the shockwave effect on collagens. *Spectrochim. Acta Part. A* **2012**, *86*, 360–365. [CrossRef]

46. Czerniecka-Kubicka, A.; Neilsen, G.; Dickson, M.S.; Woodfield, B.F.; Janus-Kubiak, M.; Kubisz, L.; Zarzyka, I.; Zielecki, W.; Skotnicki, M.; Hojan-Jezierska, D.; et al. Vibrational heat capacity of silver carp collagen. *Int. J. Biol. Macromol.* **2020**, *163*, 833–841.

47. Kubisz, L.; Hojan-Jezierska, D. Application of in vivo electrical impedance measurement in human skin assessment. In Proceedings of the 1st International Conference on Chemistry for Beauty and Health, BEAUTY—TORUŃ, Torun, Poland, 13–16 June 2018.

48. Meyer, M. Processing of collagen based biomaterials and the resulting materials properties. *Biomed. Eng. Online* **2019**, *18*, 1–74. [CrossRef]

49. Sionkowska, A.; Lewandowska, K.; Adamiak, K. The Influence of UV Light on Rheological Properties of Collagen Extracted from Silver Carp Skin. *Materials* **2020**, *13*, 4453. [CrossRef]

50. Gauza-Włodarczyk, M.; Kubisz, L.; Włodarczyk, D. Amino acid composition in determination of collagen origin and assessment of physical factors effects. *Int. J. Biol. Macromol.* **2017**, *104*, 987–991. [CrossRef] [PubMed]

51. Wiliams, R.W.; Dunker, A.K. Determination of the secondary structure of proteins from the Amide I band of the laser Raman spectrum. *J. Mol. Biol.* **1981**, *152*, 783–813. [CrossRef]

52. Wiliams, R.W. Estimation of protein secondary structure from the laser Raman amide I spectrum. *J. Mol. Biol.* **1983**, *166*, 581–603. [CrossRef]

53. Alix, A.J.P.; Pedanou, G.; Berjot, M. Fast determination of the quantitative secondary structure of proteins by using some parameters of the Raman amide I band. *J. Mol. Struct.* **1988**, *174*, 159–164. [CrossRef]

54. Edwards, H.G.M.; Farwell, D.W.; Holder, J.M.; Lawson, E.E. Fourier-tranform Raman spectroscopy of ivory: II.Spectroscopic analysis and assignments. *J. Mol. Str.* **1997**, *435*, 49–58. [CrossRef]

55. Cai, S.; Singh, B.R. Identification of β-turn and random coil amide III infrared bands for secondary structure estimation of proteins. *Biophys. Chem.* **1999**, *80*, 7–20. [CrossRef]

56. Ignatiewa, N.; Zakharkina, O.; Leroy, G.; Sobol, E.; Vorobiewa, N.; Mordon, S. Molecular processes and structural alterations in laser reshaping of cartilage. *Laser Phys. Lett.* **2007**, *4*, 749–753. [CrossRef]

57. Janko, M.; Davydovskaya, P.; Bauer, M.; Zink, A.; Stark, R.W. Anisotropic Raman scattering in collagen bundles. *Optics Lett.* **2010**, *35*, 2765–2767. [CrossRef] [PubMed]

58. Mandal, A.; Sekar, S.; Chandrasekaran, N.; Mukherjee, A.; Sastry, T.P. Vibrational spectroscopic investigation on interaction of sago starch capped silver nanoparticles with collagen: A comparative physicochemical study using FT-IR and FT-Raman techniques. *RSC Adv.* **2015**, *5*, 15763–15771. [CrossRef]

59. Knudsen, L.; Johansson, C.K.; Philipsen, P.A.; Gniadecka, M.; Wulf, H.C. Natural vibrations and reproducibility of in vivo near-infrared Fourier transform Raman spectroscopy of normal human skin. *J. Raman Spectrosc.* **2002**, *33*, 574–579. [CrossRef]

60. Fernandes, R.M.T.; Neto, R.G.C.; Paschoal, C.W.A.; Rohling, J.H.; Bezerra, C.W.B. Collagen films from swim bladders: Preparation method and properties. *Colloids Surf. B Biointerfaces* **2008**, *62*, 17–21. [CrossRef] [PubMed]

61. Safandowska, M.; Pietrucha, K. Effect of fish collagen modification on its thermal and rheological properties. *Int. J. Biol. Macromol.* **2013**, *53*, 32–37. [CrossRef]

62. Pietrucha, K.; Safandowska, M. Dialdehyde cellulose-crosslinked collagen and its physicochemical properties. *Process. Biochem.* **2015**, *50*, 2105–2111. [CrossRef]